

Seeing the Atomic Orbital: First-Principles Study of the Effect of Tip Termination on Atomic Force Microscopy

Minghuang Huang,¹ Martin Čuma,² and Feng Liu^{1,*}

¹Department of Materials Science and Engineering, University of Utah, Salt Lake City, Utah 84112, USA

²Center for High Performance Computing, University of Utah, Salt Lake City, Utah 84112, USA

(Received 3 December 2002; published 23 June 2003)

We perform extensive first-principles calculations to simulate the topographical atomic-force-microscope image of an adatom on the Si(111)-(7 × 7) surface, demonstrating the feasibility of imaging not only the atoms but also the atomic orbitals. Our comparative study of tip terminations shows that two subatomic features can appear for a single adatom when it is imaged by a Si(001)-type tip having two dangling bonds on its apex, while only one feature would appear if it were imaged by a Si(111)-type tip having one dangling bond on the apex. The key condition for seeing the atomic orbitals is to bring the tip so close to the surface that the angular-dependent force dominates the tip-surface interaction.

DOI: 10.1103/PhysRevLett.90.256101

PACS numbers: 68.37.Ps, 07.79.Lh, 71.15.-m

The invention of scanning tunneling microscopy (STM) [1] and atomic force microscopy (AFM) [2] has allowed imaging of surfaces with atomic resolution. The first atomically resolved AFM image of a reactive surface was achieved on Si(111)-(7 × 7) by Giessibl [3] using frequency-modulation (FM) AFM under ultrahigh vacuum. Recent improvements have made the quality of AFM images comparable to STM [4–9]. However, interpretation of STM or AFM images is not simple and often must be aided by first-principles calculations [10–12]. This is because the atomic imaging is inherently “indirect,” by means of surface electron density in STM and interatomic interactions in AFM. Furthermore, the image features depend strongly upon the nature of the tip [9,13], making the interpretation even more complicated.

In general, the force between tip and surface in AFM is assumed to be only distance (radial)-dependent. Surprisingly, Giessibl *et al.* observed two crescents on a single adatom on the Si(111)-(7 × 7) surface [6] and suggested that such subatomic features reflect a tip apex with two dangling bonds interacting with surface adatom with angular-dependent force. However, such a possibility was questioned by Hug *et al.* [14] who suggested that artifacts of the imaging process might have engendered the image features that were interpreted as subatomic features, and the subject remains controversial [7–9,14,15]. One of the major uncertainties arises from the fact that the interpretation of AFM image relies critically upon its comparison with a theoretically simulated image, and all previous simulations [6,15–17] are based on empirical potentials that may not be fully correct. Furthermore, subatomic features are observed only in some experiments [6], and not in others [7–9]. Consequently, if atomic orbitals can be indeed imaged, the requisite conditions for the AFM tip and the operational mode must be established in order to guide and evaluate such experiments.

To resolve the controversy and, more importantly, to establish the feasibility of AFM imaging of atomic orbi-

tals through angular-dependent force, we perform extensive first-principles calculations to directly simulate topographical FM-AFM images of an adatom on Si(111)-(7 × 7). Our comparative study of tip terminations demonstrates that subatomic features can appear only for a Si(001)-type tip having two dangling bonds on its apex atom, while, in every case, only a single feature appears for a Si(111)-type tip having one dangling bond on the apex atom. We show that in order to image the atomic orbitals, the tip needs to be brought closer to the surface—within the range of atomic bonding—where angular-dependent forces dominate the interaction between the tip and the surface.

We simulate topographical FM-AFM images of an adatom on Si(111)-(7 × 7), using the first-principles density-functional pseudopotential plane-wave method [18]. The supercell consists of a Si tip positioned above a Si(111)-(7 × 7) slab, as shown in Fig. 1. Two different tips are considered: one of the Si(001) termination with its apex atom having two dangling bonds pointing toward the surface and the other of the Si(111) termination with its apex atom having one dangling bond pointing toward

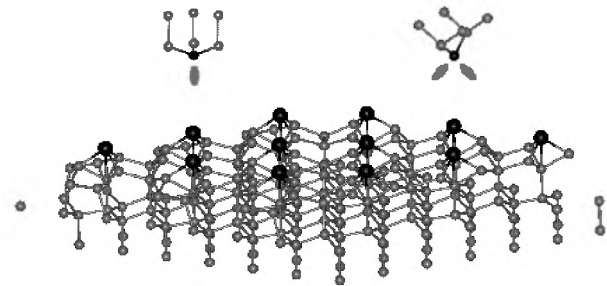


FIG. 1. Ball-and-stick model of two tips [Si(001) tip on the right and Si(111) on the left] and Si(111)-(7 × 7) surface. Surface adatoms are emphasized as bigger black balls. Dangling bonds on the tip apex atom are indicated. Only one tip is placed above one of the surface adatoms at a time in the simulation.

the surface (Fig. 1). Each tip, as a bulk fragment, is made up of seven atoms, which is the minimum number required for the apex atom and its immediate neighbors to mimic the sp^3 hybridization in the bulk.

The dimensions of the supercell are $26.9 \times 26.9 \times 25.0$ Å, containing a total of 256 atoms. We use a plane-wave cutoff energy of 10 Ryd and a single Γ k point for Brillouin zone sampling. To simulate the AFM image, we scan the tip laterally above an adatom over a $3 \text{ Å} \times 3 \text{ Å}$ area at $49 (7 \times 7)$ grid points (insets of Fig. 2); at each grid point, we scan vertically from $z = 4.5$ Å to 2.0 Å with a 0.5 Å step. Total energy is minimized using the conjugate gradient method, converged to 1×10^{-5} eV/atom. During the scan, atoms in the top four layers of the slab are fully relaxed, while the bottom two layers are fixed at bulk positions. The atoms in the tip are kept fixed, resembling a super stiff tip [6,19] and maintaining the distinctive geometric character of each tip.

The tip-surface interaction involves both a short-range chemical-bonding interaction and a long-range Van der Waals interaction. Previous first-principles calculations [10,11] have shown that the short-range bonding interaction is responsible for achieving atomic resolution. Using a Si(111)-type tip, Pérez *et al.* [10] show that even at a tip-surface distance of 5 Å, the interaction between the dangling bonds on the tip apex atom and the surface adatom accounts for 85% of the total frequency shift. The frequency shift, $\Delta f = (f_0/kA^{3/2})\gamma$ [6]. f_0 is eigenfrequency, k is spring constant, A is oscillation amplitude, and γ is the normalized frequency shift, which is calculated from the force gradient using the large oscillation amplitude approximation [16] as

$$\gamma(z) = \int_0^\infty \frac{F_{ts}(z_m + z)}{\pi\sqrt{2z}} dz. \quad (1)$$

F_{ts} is the tip-surface force, z_m is the minimum tip-surface distance, and z is the vertical tip position during oscillation. Ideally, one would like to use a fine vertical grid to calculate force from first principles, but it would be computationally too demanding. Instead, we calculate the tip-

surface interaction energy every 0.5 Å from $z = 4.5$ Å to 2.0 Å, and fit the calculated data with an analytical function of Morse potential,

$$V(z) = V_0 \left\{ \left[1 - \exp\left(-2b \frac{z - z_c}{z_c}\right) \right]^2 - 1 \right\} + C. \quad (2)$$

$V(z)$ is the interaction energy as a function of the “tip-surface” distance z , which is defined as the distance before relaxation. Parameters z_c , b , and V_0 are related to the strength and extent of the two-body bonding interaction. C is a constant related to the zero-point energy but can be chosen arbitrarily as it is irrelevant to force calculation. Thus, the force gradient can be obtained analytically from the derivative of the fitted Morse potential of Eq. (2).

We are able to fit very nicely all the 49 potential-energy curves at each in-plane grid point for both tips. Figure 2 shows two typical potential-energy curves of the Si(001) tip-surface interaction. When the tip apex atom is right above the surface adatom, at the in-plane grid point of $(0.0, 0.0)$ [Fig. 2(a)], the tip-surface interaction has both an attractive and a repulsive range from $z = 4.5$ Å to 2.0 Å and exhibits a minimum at $z \sim 2.30$ Å, which corresponds to the bond length in bulk silicon. In contrast, when the tip apex atom is farther away from the surface adatom, such as at the in-plane grid point of $(1.5 \text{ Å}, 1.5 \text{ Å})$ [Fig. 2(b)], the tip-surface interaction is only attractive from $z = 4.5$ Å to 2.0 Å.

Using two sets of 49 potential-energy curves, we calculate the normalized frequency shift at each in-plane grid point and simulate the AFM image of the adatom for each type of tip termination. First, to investigate how the nature of tip-surface interaction changes with tip-surface distance, we simulate constant-height (CH) images (Fig. 3), using different (minimum) tip-surface distances, z_m . The images evolve in qualitatively different manners for the Si(001) tip (left panel) and the Si(111) tip (right panel). The Si(001)-tip images change dramatically with a decreasing tip-surface distance: when $z_m > 2.5$ Å, only one maximum (frequency shift) appears in the image;

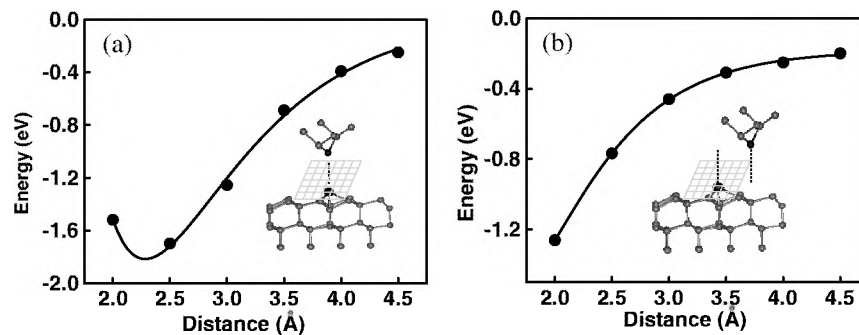


FIG. 2. Interaction energy (eV) vs tip-surface distance, z (Å), for the Si(001) tip. Lines are Morse-potential fits to the calculated data (solid dots). The insets show the (7×7) , $3 \text{ Å} \times 3 \text{ Å}$ in-plane grid (enlarged) for the lateral scan above the adatom. (a) The tip is right above adatom at the in-plane grid point, $(0.0, 0.0)$. (b) The tip is away from adatom at the in-plane grid point, $(1.5 \text{ Å}, 1.5 \text{ Å})$.

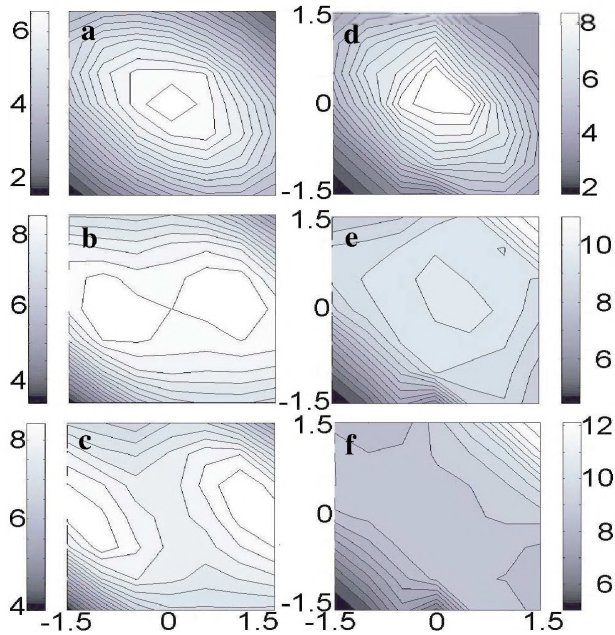


FIG. 3 (color online). Simulated constant-height FM-AFM images at three different heights of $z_m = 3.10$, 2.40 , and 2.30 Å. The normalized frequency shifts ($f/\text{Nm}^{1/2}$) are indicated by the bar next to image. The left panel is for Si(001) tip: (a) at $z_m = 3.10$ Å, a single maximum; (b) at $z_m = 2.40$ Å, two maxima separated by ~ 1.5 Å; (c) at $z_m = 2.30$ Å, two most pronounced maxima separated by ~ 2.5 Å. The right panel is for Si(111) tip: at all distances, only one maximum with its position shifted from the center (d) to the upper-right corner (e),(f).

when $z_m < 2.4$ Å, two maxima appear in the image. In contrast, the Si(111)-tip images remain qualitatively the same with only one maximum appearing at any tip-surface distance [20].

The CH images in Fig. 3 demonstrate that the nature of tip-surface interaction changes qualitatively with a decreasing tip-surface distance for the Si(001) tip. At long distances, the tip-surface interaction, or more precisely, the dangling bond–dangling bond interaction, is only radial dependent; while at short distances, it becomes angular dependent [21]. Because there are two dangling bonds on the tip apex, the angular dependence gradually yields two maxima in the CH image with a decreasing tip-surface distance, and they become most pronounced at $z_m = 2.30$ Å, corresponding to the bond length in the bulk Si.

This result confirms Ref. [6] results and can be used to explain the observed subatomic features [6]. However, this result has been questioned [14] because the experimental images are topographic (constant frequency). Furthermore, the frequency shift due to the chemical-bonding interaction is about 10 Hz, as shown in Fig. 3, which agrees with previous theoretical values [6,10,15,16]. But the frequency shift used in the experiment is about 140–160 Hz [6]. Thus, to compare directly

with the experiment, we next simulate topographic imaging using the experimentally chosen range of frequency shift.

Inclusion of long-range Van der Waals interaction would increase the frequency shift, but only by ~ 2 Hz [10], which is insignificant here. The large frequency shift of ~ 150 Hz occurs in the experiment [6] because a large bias ($+1.6$ V) is applied between the tip and the surface, contributing a large electrostatic force. Thus, we add an additional electrostatic interaction [16]. Figure 4 shows our simulated topographic images at three constant-frequency shifts of -140 , -150 , and -160 Hz, for the Si(001) and Si(111) tips in the left and right panels, respectively. Again, similar to the CH images (Fig. 3), the topographic images are qualitatively different for the two tips. For the Si(001) tip, at the relatively smaller frequency shift of $\Delta f = -140$ Hz [Fig. 4(a)], only one maximum appears in the image, whereas at the larger frequency shift of $\Delta f = -160$ Hz [Fig. 4(c)], two maxima emerge. For the Si(111) tip, however, only one maximum appears for all frequency shifts [Figs. 4(d)–4(f)].

A close correlation is evident between the CH images (Fig. 3) and the topographic images (Fig. 4). This correlation indicates that, as in the CH images, the physical genesis of the double maxima appearing in the

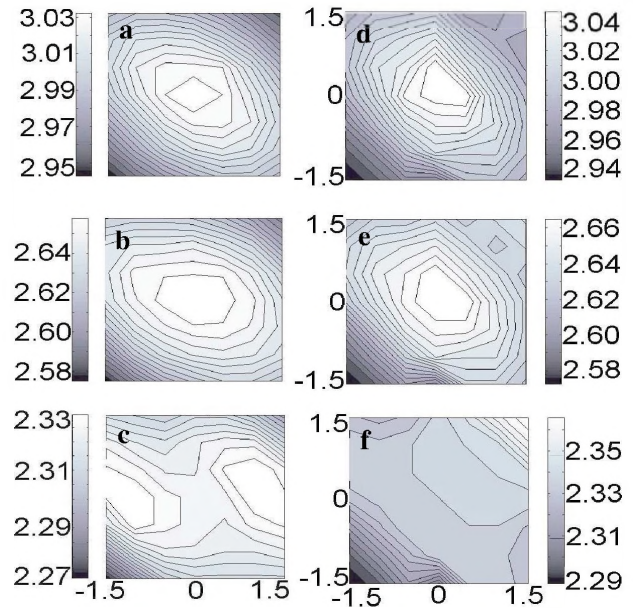


FIG. 4 (color online). Simulated topographical FM-AFM images at three different frequency shifts (Δf), calculated using $f_0 = 16860$ Hz, $k = 1800$ N/m, and $A = 8$ Å [6]. Height variations (Å) are indicated by the bar next to image. The left panel is for Si(001) tip: (a) at $\Delta f = -140$ Hz, a single maximum; (b) at $\Delta f = -150$ Hz, still a single maximum but with extended maximum area; (c) at $\Delta f = -160$ Hz, two maxima separated by ~ 2.0 Å. The right panel is for Si(111) tip: at all frequency shifts, only one maximum with its position shifted from the center (d),(e) to the upper-right corner (f).

topographic image [Fig. 4(c)] is attributable to the two dangling bonds on the Si(001) tip apex, even though the greatest portion of the frequency shift is produced by the electrostatic force rather than the chemical-bonding force. The topographic image at $\Delta f = -140$ Hz [Fig. 4(a)] shows that the vertically scanned tip-surface distance is relatively long, ranging from ~ 2.90 – 3.15 Å. Consequently, the image displays only one maximum, in accordance with the CH image for the same distance range [Fig. 3(a)]. In contrast, at $\Delta f = -160$ Hz [Fig. 4(c)], the vertically scanned minimum tip-surface distance is much shorter, ranging from ~ 2.25 – 2.37 Å. Consequently, two maxima appear, in accordance with the CH image at $z_m = 2.30$ Å [Fig. 3(c)].

The above analyses show that it is indeed possible to resolve the number of atomic orbitals (dangling bonds) on the tip apex (or equivalently, on the surface atom) by AFM. To achieve this, the critical condition for AFM operation is to bring the tip rather close to the surface, in the range of atomic bonding, where the angular-dependent force dominates the tip-surface interaction and hence, the image. This may explain why subatomic features are observed only in some experiments [6] but not in others [7–9]. One major difference is that the experiment [6] that found subatomic features operated under a large bias (+1.6 V), which pushed the tip closer to the surface reaching the angular-dependent bonding range of ~ 2.3 Å; while other experiments [7–9], presumably using a Si(001) tip (Of course, a Si(111) tip would never reveal subatomic features.), have operated either without bias or with a small bias such as +0.2 V [9], so the tip-surface distance is noticeably longer and beyond the angular-dependent range of interaction.

In principle, AFM should be capable of imaging not only the number of atomic orbitals on an atom, but also the extent and orientation of the atomic orbitals. For example, the distance between the two maxima in the topographic image of Fig. 4(c) is ~ 2 Å, which agrees well with the experiment [6]. Physically, it should represent the extent and angle of the two dangling bonds on the apex atom of the Si(001) tip. As the distance between the two maxima in an image depends on the frequency shift used to produce the image, it might be possible to map out detailed dangling-bond terminations by imaging with a series of frequency shifts.

In conclusion, we have performed extensive first-principles simulation of topographic FM-AFM imaging of an adatom on Si(111)-(7 × 7), demonstrating from first principles the feasibility of AFM imaging of atomic orbitals. Our comparative study of tip terminations confirms that AFM is capable of resolving two dangling bonds on the apex of a Si(001) tip vs one dangling bond on a Si(111) tip. The critical condition for AFM operation to resolve the atomic orbitals is to bring the tip very close to the surface—within the range of atomic bonding—so that the angular-dependent forces resulting from the

atomic-orbital orientations participate in the tip-surface interaction and hence become apparent in the images.

This work is partly supported by DOE, Grant No. DE-FG03-01ER45875.

*Corresponding author.

Electronic address: fliu@eng.utah.edu

- [1] G. Binnig, H. Rohrer, Ch. Gerber, and E. Weibel, *Phys. Rev. Lett.* **50**, 120 (1983).
- [2] G. Binnig, C. F. Quate, and Ch. Gerber, *Phys. Rev. Lett.* **56**, 930 (1986).
- [3] F. J. Giessibl, *Science* **267**, 68 (1995).
- [4] S. Kitamura and M. Iwatsuki, *Jpn. J. Appl. Phys.* **35**, L145 (1995).
- [5] H. Ueyama, M. Ohta, Y. Sugawara, and S. Morita, *Jpn. J. Appl. Phys.* **34**, L1086 (1995).
- [6] Giessibl *et al.*, *Science* **289**, 422 (2000).
- [7] T. Uchihashi *et al.*, *Phys. Rev. B* **56**, 9834 (1997).
- [8] M. A. Lanz *et al.*, *Phys. Rev. Lett.* **84**, 2642 (2000).
- [9] T. Eguchi and Y. Hasegawa, *Phys. Rev. Lett.* **89**, 266105 (2002).
- [10] R. Pérez, M. C. Payne, I. Štich, and K. Terakura, *Phys. Rev. Lett.* **78**, 678 (1997); *Phys. Rev. B* **58**, 10835 (1998).
- [11] N. Sasaki, S. Watanabe, and M. Tsukada, *Phys. Rev. Lett.* **88**, 046106 (2002).
- [12] Z.-Y. Lu *et al.*, *Phys. Rev. Lett.* **85**, 5603 (2000).
- [13] J. R. Hahn and W. Ho, *Phys. Rev. Lett.* **87**, 196102 (2001).
- [14] H. J. Hug *et al.*, *Science* **291**, 2509a (2001).
- [15] Giessibl *et al.*, *Science* **291**, 2509a (2001).
- [16] The electrostatic force is approximated as $f_e(z) = -(\pi\epsilon_0RV^2/z)$, by assuming a bias voltage of V applied between a spherical tip of radius R and a flat surface [F. J. Giessibl and H. Bielefeldt, *Phys. Rev. B* **61**, 9968 (2000)]. We choose a radius R to make the total frequency shift fall into the experimental range.
- [17] F. J. Giessibl *et al.*, *Ann. Phys. (Leipzig)* **10**, 11 (2001).
- [18] M. C. Payne *et al.*, *Rev. Mod. Phys.* **64**, 1045 (1992).
- [19] F. J. Giessibl, *Appl. Phys. Lett.* **76**, 1470 (2000).
- [20] The position of the maximum actually shifts from the image's center [$z_m = 3.1$ Å, Fig. 3(d)] to the upper-right corner [$z_m = 2.3$ Å, Fig. 3(f)]. This is because in the Si(111) tip, the vertical separation between the apex atom and its three nearest neighbors is ~ 0.78 Å. Consequently, its neighbors can also interact with the surface adatom when the tip-surface distance is short. Because of the specific tip orientation used with respect to the surface, it turns out when the tip is placed at the upper-right corner of the in-plane grid, the interaction between one of the neighbors and the adatom becomes the dominating interaction at a short tip-surface distance, causing the shift of the maximum from the center [Fig. 3(d)] to the upper-right corner [Figs. 3(c) and 3(e)]. Looking carefully at Fig. 3(e), there is actually a very weak second maximum at the center.
- [21] The angular dependence, resulted from symmetries (angular momentum) of atomic orbitals of tip apex, has also been shown for STM; C. J. Chen, *Phys. Rev. Lett.* **69**, 1656 (1992).